Solar Energy Materials & Solar Cells 94 (2010) 1179–1184

Contents lists available at ScienceDirect

Solar Energy Materials & Solar Cells

journal homepage: www.elsevier.com/locate/solmat

Letter

Transparent Cu nanowire mesh electrode on flexible substrates fabricated by transfer printing and its application in organic solar cells

Myung-Gyu Kang [a], Hui Joon Park [b], Se Hyun Ahn [c], L. Jay Guo [a,*]

[a] Department of Electrical Engineering and Computer Science, The University of Michigan, 1301 Beal Ave., Ann Arbor, MI 48109, USA
[b] Macromolecular Science and Engineering, The University of Michigan, 2300 Hayward St., Ann Arbor, MI 48109, USA
[c] Department of Mechanical Engineering, The University of Michigan, 2350 Hayward St., Ann Arbor, MI 48109, USA

ARTICLE INFO

Article history:
Received 10 January 2010
Received in revised form
23 February 2010
Accepted 25 February 2010
Available online 24 March 2010

Keywords:
Transparent metal electrode
PDMS
Nanoimprint lithography (NIL)
Roll-to-roll nanoimprint lithography (R2RNIL)
Organic solar cell

ABSTRACT

We report the flexible transparent Cu nanowire mesh electrode fabricated by simple transfer printing from flexible PDMS stamp as a potential replacement for the conventional ITO electrode in organic solar cell applications. Fabricated Cu mesh electrode shows a greater flexibility than conventional ITO electrode deposited on plastic substrates, and exhibits high optical transmittance and electrical conductance. It can be bent to 3 mm radius of curvature with no degradation of the conductance. Large area nanoscale metal electrodes on flexible substrates are demonstrated using a roll-to-roll process. The organic solar cell made with the transparent Cu electrode performs as good as the one with ITO electrode, which indicates that such electrode has the potential to replace conventional ITO electrode for low-cost, large-area flexible organic solar cell applications.

1. Introduction

Organic solar cells (OSCs) offer a promising alternative to inorganic solar cells due to their low cost, easy fabrication, and compatibility with flexible substrates over large areas [1–5]. In particular, flexible OSCs [6] have potentials to apply to packaging, clothing, flexible screens, and recharging small mobile electronics. Recently, significant advances have been made for the realization of low-cost and large-area flexible OSCs by focusing on the materials and processing methods [7,8]. The possibility of mass production of flexible OSCs using roll-to-roll fabrication has also been demonstrated by Krebs et al. [9]. Most of the organic solar cells have been made on indium tin oxide (ITO) substrate because ITO offers transparency in the visible range of the electromagnetic spectrum as well as electrical conductivity. Therefore, current high performance organic solar cells are mostly fabricated on ITO electrode [10–15]. However, ITO is not the best choice for low-cost and high-performance flexible OSC applications, because the high quality ITO, especially high conductivity, requires high temperature annealing, which is incompatible with plastic-based flexible substrates. The poor conductivity of the ITO film on flexible substrates reduces the fill-factor (FF) of the device resulting in low power conversion efficiency of large area OSCs [16]. The rather brittle ITO film is also not sufficient for flexible applications. In fact, the poor mechanical stability of ITO can cause device failure when the ITO-coated flexible substrate is bent [16–18]. Moreover, the price of ITO drastically increases due to the limited supply of the indium element and the increasing demand from the rapidly expanding display market. These aspects of ITO potentially prevent the realization of low-cost and high-performance large scale OSC fabrication. Several alternative materials as transparent conductive electrode (TCE) including carbon nanotube networks [18–21], conductive polymers [22–24], and random Ag nanowire mesh [25] have been recently investigated and showed adequate performance. However, they suffer from either low conductivity or high surface roughness, which cause reduced FF and power conversion efficiency. We have recently developed another type of TCE based on periodic metallic nanostructures on glass substrates using nanoimprint lithography (NIL) and demonstrated that high optical transmittance and high electrical conductivity could be achieved at the same time by controlling the line-width and the thickness of the metallic nanostructures [26]. Specifically, it has been shown that conductivity of such transparent metal electrode was enhanced by a factor of three at the cost of a small decrease in optical transmittance by just doubling the metal thickness. The high conductivity of TCE is one of the most important parameters for high-performance large area organic solar cell applications. It is

* Corresponding author. Tel.: +1 734 647 7718; fax: +1 734 763 9324.
E-mail address: guo@eecs.umich.edu (L. Jay Guo).

0927-0248/$ - see front matter © 2010 Elsevier B.V. All rights reserved.
doi:10.1016/j.solmat.2010.02.039

also easily anticipated that the performance of the transparent metal electrode does not depend on the kinds of the substrate because such electrode does not require another processing to enhance its performance such as high temperature annealing needed for high performance ITO. One requirement for realizing transparent metal electrode on flexible substrates is to develop efficient nanofabrication technique because the NIL used for glass substrate requires high temperature and pressure, which are not compatible with flexible substrates. Therefore, in this paper, we demonstrate a transparent Cu nanowire mesh electrode on polyethylene terephthalate (PET) substrate by simple transfer printing from flexible poly(dimethylsiloxane) (PDMS) stamp. The fabricated transparent Cu electrode shows optical transmittance comparable to the ITO electrode in the visible range, but a lower sheet resistance (R_{sh}) than that of typical ITO electrode. Moreover, it is much more flexible than the sputter-deposited ITO on plastic substrate, and can be bent to ~3 mm radius of curvature with no degradation of the conductance. We also demonstrate the potential of large area fabrication of such transparent metal electrode using a roll-to-roll process. Organic solar cells made with the Cu mesh electrode performs as good as those made with conventional ITO electrode, which indicates that the transparent Cu electrode can potentially replace the ITO electrode with better flexibility and lower cost.

2. Experimental

2.1. Nanoscale metal transfer printing using PDMS stamp

Fig. 1 shows the schematic diagram of the fabrication of the PDMS stamp and the transfer printing of Cu nanowire mesh electrode using the PDMS stamp. Nanoimprint lithography (NIL) [27] was first performed to fabricate the resist template (MRI-8030, Microresist Technology GmbH) required for the fabrication of the PDMS stamp. The SiO_2 mold (Fig. 2(a)) for NIL consists of two sets of orthogonally oriented grating structures with a depth of 130 nm but with different periods. One grating has a period of 700 nm and a line-width of 70 nm, and the other 10 μm period and a line-width of 400 nm [26,28]. The PDMS stamp was fabricated from the imprinted resist template by drop-casting and curing [28,29]. The stamp is made of two different PDMS materials. High modulus PDMS was first drop-casted and cured at 65 °C for 5 min to faithfully replicate the nanoscale features [30]. Next commercial PDMS, sylgard 184, was drop-casted and cured at 65 °C for 2 h on top of the high modulus PDMS layer to provide the flexible mechanical support to the patterned layer. After removing the PDMS stamp from the resist template, 40 nm thick Cu and 2 nm thick Ti were sequentially deposited on the PDMS stamp by electron-beam evaporation at a rate of 2 Å/s. After a brief O_2 plasma treatment of the Cu/Ti layer, the metal was transferred on to a 30 nm thick poly(3,4-ethylenedioxythiophene):poly(styrenesulfonate) (PEDOT:PSS) layer spin coated on PET substrate under a

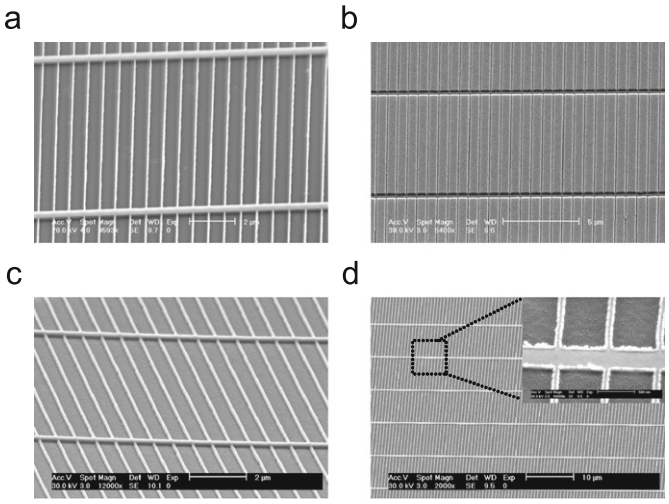

Fig. 2. SEM images of (a) the SiO_2 mold for NIL, (b) the imprinted resist template, (c) the fabricated PDMS stamp, and (d) the transferred Cu mesh electrode onto PEDOT:PSS coated PET substrate.

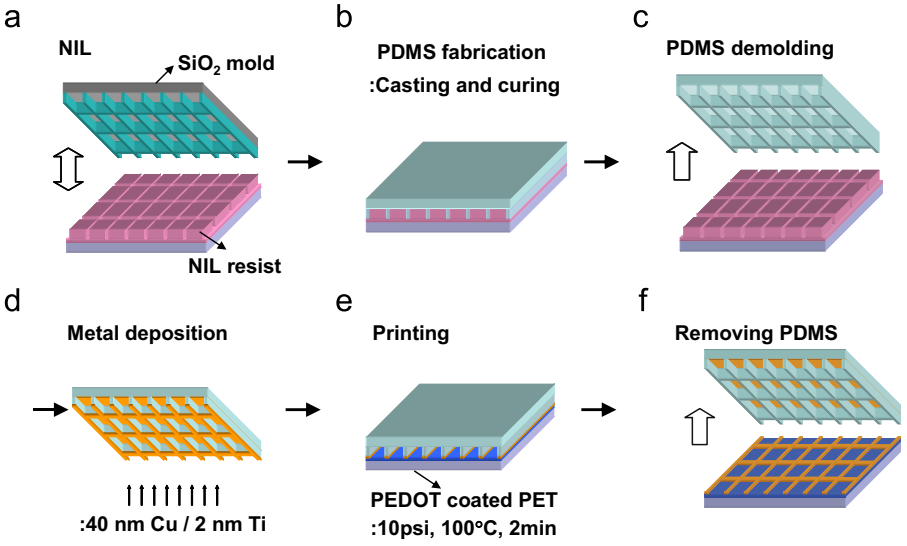

Fig. 1. Schematic diagram of the fabrication of the PDMS stamp and the transfer printing of Cu nanowire mesh electrode. (a) The conventional NIL produces the resist template. (b) The PDMSs are drop-casted and cured. High modulus PDMS is first drop-casted and cured at 65 °C for 5 min. The commercial PDMS, sylgard 184, is then drop-casted and cured at 65 °C for 2 h to mechanically support the first layer. (c) The PDMS is demolded after cooling down to room temperature. (d) 40 nm thick Cu and 2 nm thick Ti are sequentially deposited by electron-beam evaporation. (e) The Cu mesh on the PDMS stamp is transferred onto PEDOT:PSS coated PET substrate at 10 psi and 100 °C for 2 min. (f) Lifting up the PDMS stamp leaves the Cu mesh electrode on PEDOT:PSS coated PET substrate.

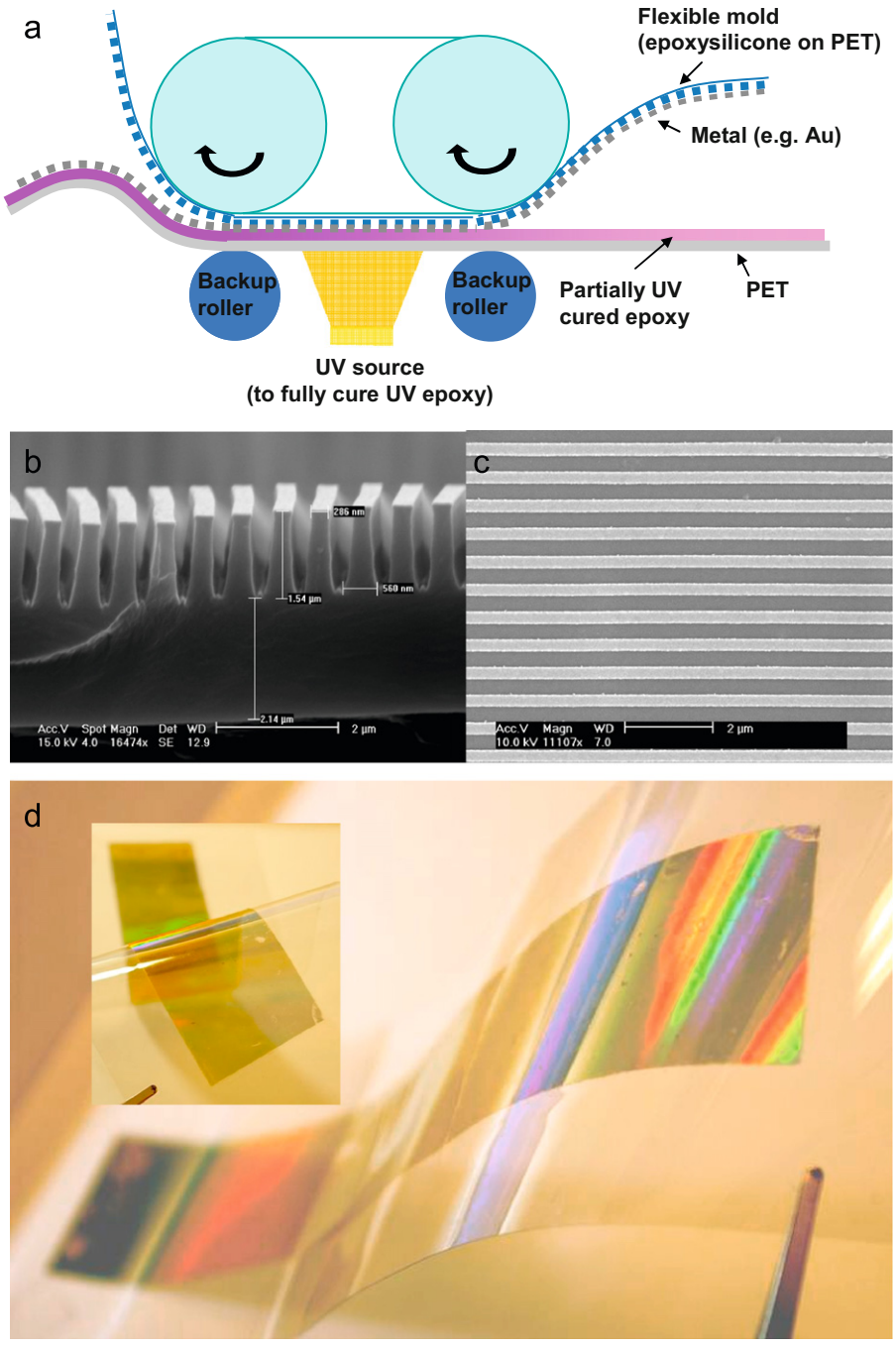

Fig. 3. (a) Schematic of the R2R transfer printing process, (b) SEM images of the imprinted epoxysilicon grating structure on the replicated flexible mold, (c) the transferred Au nanograting on UV-cured epoxy coated on a PET substrate, and (d) photograph of large area (32 mm × 184 mm) Au nanogratings on UV epoxy coated PET substrate. Inset photograph shows the transparency of the Au nanogratings transferred to PET.

pressure of 10 psi and a temperature of 100 °C for 2 min. An amount of 0.1 wt% glycerol was added to PEDOT:PSS to prevent the pre-mature drying of the PEDOT layer prior to the transfer process. Besides Cu, other metals such as Au and Ag can also be used. We present here results obtained with Cu. Cu is well suited for practical organic solar cell applications due to its much lower cost and similar work function to ITO (ca. 4.7 eV). The period (700 nm), line-width (70 nm), and thickness (40 nm) of the Cu mesh electrode fabricated were chosen to provide sufficient optical transmittance and electrical conductance for organic solar cell applications. Those parameters are conveniently varied to meet specific transmittance and conductance [26,28]. The metal transfer process is accomplished due to the difference in adhesion strength between the PDMS/Cu and the Ti/PEDOT:PSS interfaces. Since the PDMS has low surface energy [31], the adhesion of Cu to it is poor. Moreover, the sticky surface of the unbaked PEDOT:PSS leads to a strong adhesion to the thin Ti layer during the printing process resulting in successful transfer of the Cu mesh on to the PEDOT:PSS layer. To increase the yield of the printing process, the surface of the PDMS stamp can be treated with an anti-sticking layer (e.g. 1H,1H,2H,2H-perfluorodecyl trichlorosilane) before the metal evaporation. Fig. 2 shows the scanning electron micrographs (SEM) of the SiO_2 mold, the imprinted resist template, the PDMS stamp, and the transferred Cu mesh electrode on PEDOT:PSS coated PET substrate. As shown in Fig. 2(d), the large area Cu mesh pattern was uniformly transferred with high yield.

2.2. Fabrication of nanoscale metal electrode using roll-to-roll printing process

The fabrication of the nanopatterned metal electrode using the developed metal transfer printing method can potentially be extended to cost effective and large area fabrication similar to the roll-to-roll nanoimprint lithography (R2RNIL) [32,33] with the use of flexible molds. As a proof of principle, we have developed a roll-to-roll process and demonstrate nanoscale metal (e.g. Au) gratings on large area PET substrates. Fig. 3(a) shows the schematic of a continuous R2R transfer printing process. For this demonstration, surfactant (1H,1H,2H,2H-perfluorodecyl trichlorosilane) treated UV curable epoxysilicone patterns [34] with a period of 700 nm and a duty cycle of about 50% on PET substrate were used as a flexible mold (Fig. 3(b)). Here we used the mold with 50% duty cycle because we focused on demonstration of the feasibility to R2R fabrication of metal transfer printing. It is desirable to have the mold with narrow line-width for high transparency electrode. To fabricate the flexible epoxysilicone mold, a flexible fluoropolymer mold made of ethylene-tetrafluoroethylene (ETFE) [23] was first fabricated from an original large area SiO_2 mold with a period of 700 nm and duty cycle of about 50% by a thermal NIL process at 220 °C for 5 min [32]. The ETFE mold was then used to fabricate epoxysilicone mold on PET substrates by UV R2RNIL process [32] (web speed of 20 mm/s and a roller imprinting force of 220 N). An anti-sticking layer (1H,1H,2H,2H-perfluorodecyl trichlorosilane) was then thermally deposited on the fabricated epoxysilicone stamp before metal (e.g. Au) evaporation in order to reduce the adhesion of the metal layer to the mold. After a 40 nm thick Au deposition the epoxysilicone stamp was wrapped on the tensioned belt around rollers in the R2RNIL system as shown in Fig. 3(a). The Au nanogratings on the protrusions of the stamp were then transferred onto a partially cured UV epoxy (NOA72) on PET substrates in a roll-to-roll fashion. The partially cured UV epoxy on PET substrate served as an adhesion layer between the metal and the PET substrate instead of PEDOT due to the easiness of producing a uniform, large area coating on PET substrate. In this work the partially cured UV epoxy layer was prepared separately by using the same R2RNIL apparatus. NOA72 resin was uniformly coated on PET substrate using doctor blade and covered with the low-surface energy ETFE film. Rolling and low power (120 mJ/cm^2) UV exposure produced a uniform and partially cured UV resin on PET substrates, which was followed by ETFE film removal to complete the substrate preparation. The partially cured UV epoxy on PET was brought into intimate contact with the Au-coated epoxysilicone stamp under the roller pressure. The UV epoxy was fully cured by high power (2470 mJ/cm^2) UV exposure. Fig. 3(c) and (d) shows a SEM image and a photograph of the Au nanogratings on UV-cured epoxy coated on PET substrate fabricated by this technique. As shown in Fig. 3(d), large area (32 mm × 184 mm) Au nanogratings were successfully fabricated. This result implies that the fabrication of the nanopatterned metal electrode can be extended to large area continuous processing, which could help to realize low-cost and flexible transparent electrode.

2.3. Fabrication of organic solar cells

To evaluate the potential use of the fabricated transparent Cu metal electrode as a high transparency conducting electrode for organic optoelectronic devices, bulk heterojunction organic solar cells based on a blend of poly(3-hexylthiophene) (P3HT) and [6,6]-phenyl C_{61} butyric acid methyl ester (PCBM) as active materials were fabricated using such an electrode and compared to the one made with the commercial ITO electrode on PET substrate. ITO electrode on PET substrate (Sigma Aldrich, 60 Ω/□) was cleaned separately in acetone and isopropyl alcohol (IPA) under sonication for 30 min each and treated by oxygen plasma for 60 s. Filtered PEDOT:PSS purchased from H.C. Starck was then spin-coated on to each transparent electrode (Cu mesh on PEDOT coated PET and ITO on PET) at 1500 rpm for 30 s producing a 80 nm thick layer, and was then baked at 120 °C for 15 min. Next, samples were then transferred to N_2 purged glove box where a blend of P3HT and PCBM (1:1 ratio by weight) in chlorobenzene was spin-coated after filtration onto the PEDOT:PSS layer at 1000 rpm for 30 s to give a ~100 nm thick layer; and then annealed at 130 °C for 20 min. P3HT and PCBM were purchased from Rieke Metals Ltd. and American Dye source, respectively, and were used as received. Finally, thermal evaporation of a 1 nm thick LiF layer followed by a 70 nm thick Al layer through a shadow mask (diameter of 1 mm) completed the organic solar cell fabrication. Here, we used spin casting to coat the active layer uniformly as a demonstration of flexible OSC. However, other coating techniques compatible with large scale coating of active layer such as ink-jet [35], screen [36,37], gravure [38], squeezing [39], and spray [40] printing can be readily used. Current density versus voltage characteristics were measured with HP4156B semiconductor analyzer by illuminating the OSC devices with AM 1.5G simulated sun light (Oriel Solar Simulation, 100 mW/cm^2). The light intensity was calibrated by power meter (OPHIR, Nova-Oriel).

3. Results and discussion

3.1. Characteristics of the transparent Cu mesh electrode on flexible substrates

The optical transmittance of the fabricated Cu mesh electrode on PEDOT coated PET substrate in the visible wavelength range was measured and shown in Fig. 4. As a comparison, the optical transmittance of the commercial ITO coated PET (Sigma Aldrich, 60 Ω/□) was also measured and included in the figure. All the

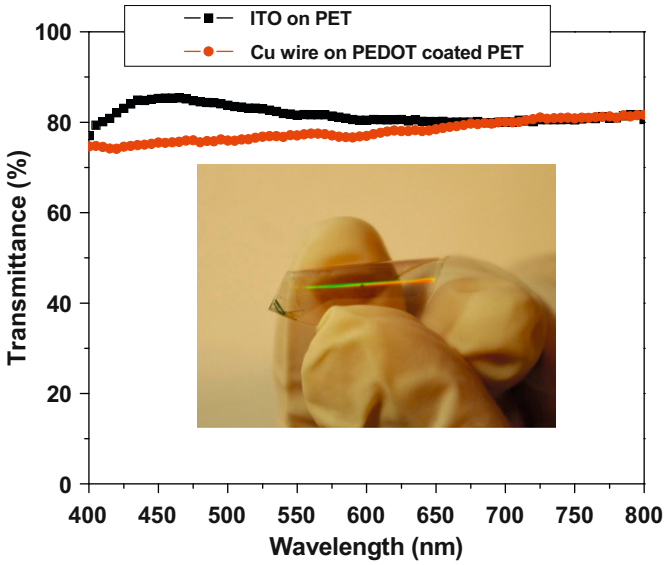

Fig. 4. Optical transmittance of 40 nm thick Cu nanowire mesh electrode with the sheet resistance of 22 Ω/□ on PEDOT coated PET substrate (●) and the commercial ITO electrode on PET substrate (60 Ω/□) (■). Inset: the photograph of the flexible Cu mesh electrode on PEDOT coated PET substrate.

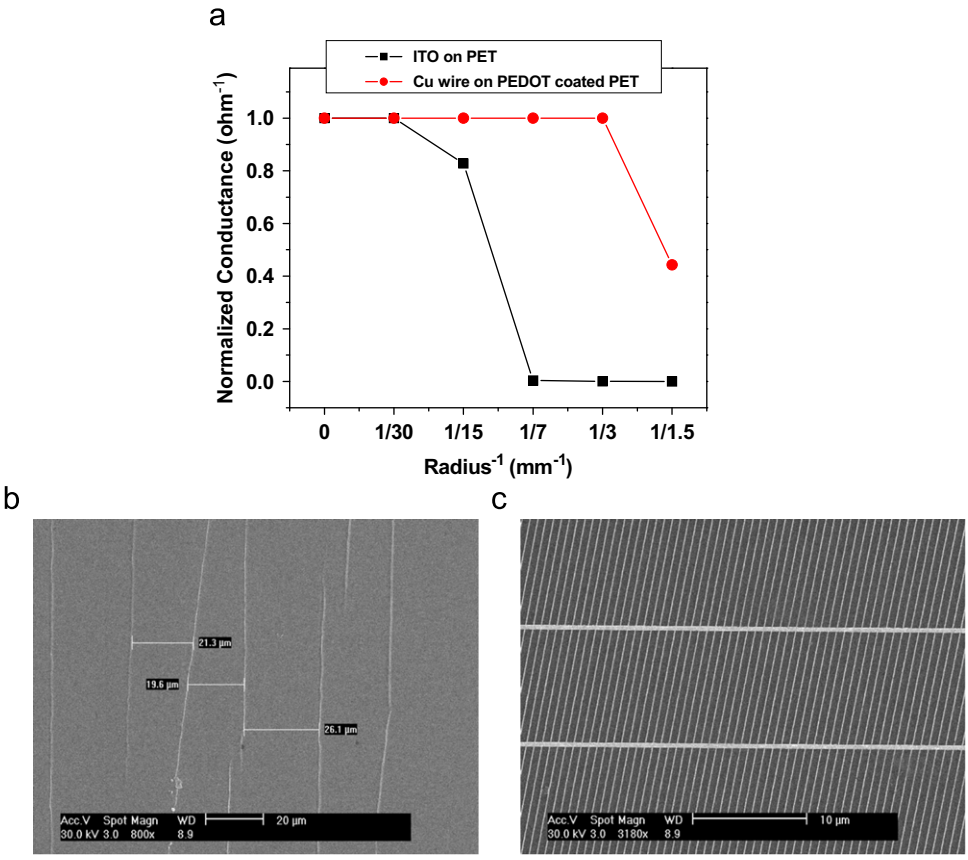

Fig. 5. (a) Normalized conductance versus inverse of the radius of curvature of the Cu wire mesh (●) and the ITO electrode (■). The Cu mesh electrode on PEDOT coated PET substrate showed a superior flexibility and can be bent to ~3 mm radius of curvature with no degradation of conductance. SEM images of the ITO (b) and Cu mesh electrode (c) after the bending test, respectively. In contrast to Cu mesh structure, the ITO severely cracked from the bending.

transmittance measurement was referenced to air. ITO has a peak transmittance of 85% at 465 nm and an average transmittance of 82% in the whole visible range. The transmittance of the Cu mesh electrode is very flat over the entire visible range and the average transmittance is about 78%. The measured sheet resistance of the transparent Cu electrode is 22 Ω/□, about three times lower than that of the ITO. Though only one set of metal line-width and thickness parameters were used in this work, our previous studies have shown that the optical transmittance and sheet resistance of the transparent metal electrode can be controlled relatively independently by adjusting the line-width and thickness of the metal grating [26]. In particular, it has been demonstrated that the sheet resistance of the transparent metal electrode was reduced by a factor of three by doubling the thickness of the metal, while the transmittance only reduces by a few percent [26,28]. In contrast, the ITO transparency will be greatly compromised if its conductivity is to be increased.

The fabricated Cu electrode was found to be much more flexible than the ITO by bending test and the results are shown in Fig. 5. In case of the transparent Cu mesh electrode, it can be bent to 3 mm radius of curvature with no degradation of the conductance. On the other hand, the conductance of the ITO started to decrease even at ~30 mm radius of curvature and dropped close to zero at ~7 mm radius. One should note that the conductance of the ITO was measured right after the specific bending radius was reached. Micro-cracking in ITO film on the order of 20 μm was observed after the bending test (Fig. 5b), which was responsible for the reduction in conductance. In contrast, the fine metal lines were intact even after the sharp bending to 3 mm radius of curvature (Fig. 5c).

3.2. *The performance of organic solar cells*

The current density (J) versus voltage (V) characteristics were measured in air by illuminating the OSC devices with AM 1.5G simulated sun light (Oriel Solar Simulator, 100 mW/cm^2). As shown in Fig. 6, the J–V characteristics of the solar cells having the transparent Cu and ITO electrode are very similar to each other, indicating that such electrodes are interchangeable. The power conversion efficiency of the device with Cu electrode, about 2.1%, is comparable to that of the device with ITO electrode, 2.24%. Both devices have similar open circuit voltage (V_{oc}) and FF which are 0.6 V and 62%, respectively. The short circuit current (J_{sc}) is 5.7 and 5.9 mA/cm^2 for the device with Cu and ITO electrode, respectively. The slight lower J_{sc} of the Cu device can be attributed to the lower transmittance of the Cu mesh electrode at the light absorption range of the active layer than that of the ITO electrode.

4. Conclusions

In summary, we have demonstrated the flexible transparent Cu nanowire mesh electrode fabricated by a simple transfer printing method using a flexible PDMS stamp. This method can be expanded to large area fabrication such as roll-to-roll process. Fabricated Cu mesh electrode showed a much greater flexibility than the conventional ITO electrode with high optical transmittance and electrical conductance. The organic solar cell made with the transparent Cu electrode worked as good as the one with the ITO electrode. For the prospect of using the transparent metal

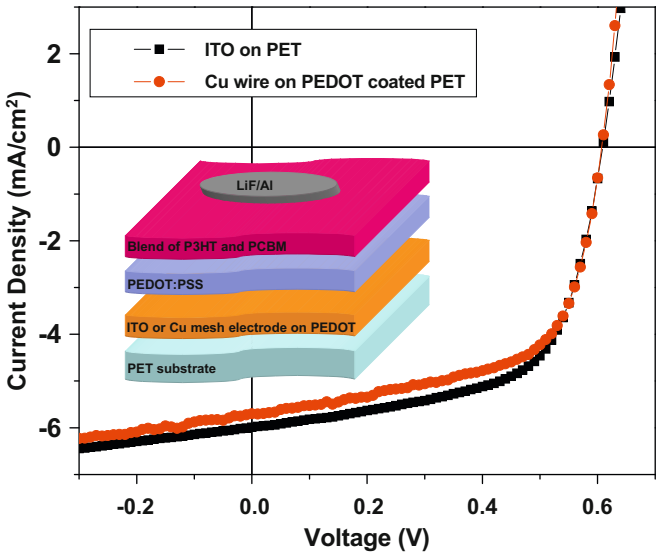

Fig. 6. *J–V* curves of devices made with transparent Cu mesh on PEDOT coated PET substrate (●) and ITO on PET substrate (■) under AM 1.5G condition. Inset: the schematic of the fabricated device showing the layer structures.

electrode to replace the conventional ITO electrode, we believe it will outperform the ITO electrode in large area solar cell application due to its superior flexibility, lower sheet resistance, and the low cost of the Cu material. It is also possible to exploit the surface plasmon enhancement effect associated with the metallic nanogratings to improve the light absorption and therefore the power efficiency of OSCs [31]. In addition, such electrode structures may find applications in other areas such as transparent electrodes for inorganic solar cells made with CIGS semiconductors, flexible OLED displays, and touch screen applications.

Acknowledgement

This work was supported in part by NSF Grant CMII 0700718 and KACST.

References

[1] C.W. Tang, Two-layer organic photovoltaic cell, Appl. Phys. Lett. 48 (1986) 183–185.
[2] G. Yu, J. Gao, J.C. Hummelen, F. Wudl, A.J. Heeger, Polymer photovoltaic cells: enhanced efficiencies via a network of internal donor–acceptor heterojunctions, Science 270 (1995) 1789–1791.
[3] P. Peumans, A. Yakimov, S.R. Forrest, Small molecular weight organic thin-film photodetectors and solar cells, J. Appl. Phys. 93 (2003) 3693–3723.
[4] S. Gunes, H. Neugebauer, N.S. Sariciftci, Conjugated polymer-based organic solar cells, Chem. Rev. 107 (2007) 1324–1338.
[5] B. Kippelen, J.-L. Brédas, Organic photovoltaics, Energy Environ. Sci. 2 (2009) 251–261.
[6] G. Dennler, N.S. Sariciftci, Flexible conjugated polymer-based plastic solar cells: from basics to applications, Proc. IEEE 93 (2005) 1429–1439.
[7] F.C. Krebs, Fabrication and processing of polymer solar cells: a review of printing and coating techniques, Sol. Energy Mater. Sol. Cells 93 (2009) 394–412.
[8] M. Helgesen, R. Søndergaard, F.C. Krebs, Advanced materials and processes for polymer solar cell devices, J. Mater. Chem. 20 (2010) 36–60.
[9] F.C. Krebs, M. Jørgensen, K. Norrman, O. Hagemann, J. Alstrup, T.D. Nielsen, J. Fyenbo, K. Larsen, J. Kristensen, A complete process for production of flexible large area polymer solar cells entirely using screen printing—first public demonstration, Sol. Energy Mater. Sol. Cells 93 (2009) 422–441.
[10] P. Peumans, S.R. Forrest, Very-high-efficiency double-heterostructure copper phthalocyanine/C[sub 60] photovoltaic cells, Appl. Phys. Lett. 79 (2001) 126–128.
[11] G. Li, V. Shrotriya, J. Huang, Y. Yao, T. Moriarty, K. Emery, Y. Yang, High-efficiency solution processable polymer photovoltaic cells by self-organization of polymer blends, Nat. Mater. 4 (2005) 864–868.
[12] W. Ma, C. Yang, X. Gong, K. Lee, A.J. Heeger, Thermally stable, efficient polymer solar cells with nanoscale control of the interpenetrating network morphology, Adv. Funct. Mater. 15 (2005) 1617–1622.
[13] J.Y. Kim, K. Lee, N.E. Coates, D. Moses, T.-Q. Nguyen, M. Dante, A.J. Heeger, Efficient tandem polymer solar cells fabricated by all-solution processing, Science 317 (2007) 222–225.
[14] F. Yang, K. Sun, S.R. Forrest, Efficient solar cells using all-organic nanocrystalline networks, Adv. Mater. 19 (2007) 4166–4171.
[15] S.H. Park, A. Roy, S. Beaupre, S. Cho, N. Coates, J.S. Moon, D. Moses, M. Leclerc, K. Lee, A.J. Heeger, Bulk heterojunction solar cells with internal quantum efficiency approaching 100%, Nat. Photon 3 (2009) 297–302.
[16] B. Maennig, J. Drechsel, D. Gebeyehu, P. Simon, F. Kozlowski, A. Werner, F. Li, S. Grundmann, S. Sonntag, M. Koch, K. Leo, M. Pfeiffer, H. Hoppe, D. Meissner, N.S. Sariciftci, I. Riedel, V. Dyakonov, J. Parisi, Organic p–i–n solar cells, Appl. Phys. A 79 (2004) 1–14.
[17] Z. Chen, B. Cotterell, W. Wang, E. Guenther, S.-J. Chua, A mechanical assessment of flexible optoelectronic devices, Thin Solid Films 394 (2001) 202–206.
[18] M.W. Rowell, M.A. Topinka, M.D. McGehee, H.-J. Prall, G. Dennler, N.S. Sariciftci, L. Hu, G. Gruner, Organic solar cells with carbon nanotube network electrodes, Appl. Phys. Lett. 88 (2006) 233506-1–233506-3.
[19] J. van de Lagemaat, T.M. Barnes, G. Rumbles, S.E. Shaheen, T.J. Coutts, C. Weeks, I. Levitsky, J. Peltola, P. Glatkowski, Organic solar cells with carbon nanotubes replacing In[sub 2]O[sub 3]:Sn as the transparent electrode, Appl. Phys. Lett. 88 (2006) 233503-1–233503-3.
[20] A.J. Miller, R.A. Hatton, S.R.P. Silva, Interpenetrating multiwall carbon nanotube electrodes for organic solar cells, Appl. Phys. Lett. 89 (2006) 133117-1–133117-3.
[21] Z. Wu, Z. Chen, X. Du, J.M. Logan, J. Sippel, M. Nikolou, K. Kamaras, J.R. Reynolds, D.B. Tanner, A.F. Hebard, A.G. Rinzler, Transparent, conductive carbon nanotube films, Science 305 (2004) 1273–1276.
[22] F. Zhang, M. Johansson, M.R. Andersson, J.C. Hummelen, O. Inganäs, Polymer photovoltaic cells with conducting polymer anodes, Adv. Mater. 14 (2002) 662–665.
[23] G.P. Kushto, W. Kim, Z.H. Kafafi, Flexible organic photovoltaics using conducting polymer electrodes, Appl. Phys. Lett. 86 (2005) 095502.
[24] S.-I. Na, S.-S. Kim, J. Jo, D.-Y. Kim, Efficient and flexible ITO-free organic solar cells using highly conductive polymer anodes, Adv. Mater. 20 (2008) 4061–4067.
[25] J.-Y. Lee, S.T. Connor, Y. Cui, P. Peumans, Solution-processed metal nanowire mesh transparent electrodes, Nano Lett. 8 (2008) 095502-1–095502-3.
[26] M.-G. Kang, L.J. Guo, Nanoimprinted semitransparent metal electrodes and their application in organic light emitting diodes, Adv. Mater. 19 (2007) 1391–1396.
[27] L.J. Guo, Nanoimprint lithography: methods and material requirements, Adv. Mater. 19 (2007) 495–513.
[28] M.-G. Kang, M.-S. Kim, J. Kim, L.J. Guo, Organic solar cells using nanoimprinted transprent metal electrodes, Adv. Mater. 20 (2008) 4408–4413.
[29] M.-G. Kang, L.J. Guo, Metal transfer assisted nanolithography on rigid and flexible substrates, J. Vac. Sci. Technol. B 26 (2008) 2421–2425.
[30] C. Pina-Hernandez, J.-S. Kim, L.J. Guo, P.-F. Fu, High-throughput and etch-selective nanoimprinting and stamping based on fast-thermal-curing poly (dimethylsiloxane)s, Adv. Mater. 19 (2007) 1222–1227.
[31] D.W.V. Krevelen, in: Properties of Polymers, Elsevier, Amsterdam, 1997.
[32] S.H. Ahn, L.J. Guo, High-speed roll-to-roll nanoimprint lithography on flexible plastic substrates, Adv. Mater. 20 (2008) 2044–2049.
[33] S.H. Ahn, L.J. Guo, Large-area roll-to-roll and roll-to-plate nanoimprint lithography and analytical models for predicting residual layer thickness, ACS Nano 3 (2009) 2304–2310.
[34] X. Cheng, L.J. Guo, P.F. Fu, Room-temperature, low-pressure nanoimprinting based on cationic photopolymerization of novel epoxysilicone monomers, Adv. Mater. 17 (2005) 1419–1424.
[35] T. Aernouts, T. Aleksandrov, C. Girotto, J. Genoe, J. Poortmans, Polymer based organic solar cells using ink-jet printed active layers, Appl. Phys. Lett. 92 (2008) 033306-1–033306-3.
[36] F.C. Krebs, H. Spanggard, T. Kjær, M. Biancardo, J. Alstrup, Large area plastic solar cell modules, Mater. Sci. Eng. B 138 (2007) 106–111.
[37] F.C. Krebs, J. Alstrup, H. Spanggaard, K. Larsen, E. Kold, Production of large-area polymer solar cells by industrial silk screen printing, lifetime considerations and lamination with polyethyleneterephthalate, Sol. Energy Mater. Sol. Cells 83 (2004) 293–300.
[38] J.M. Ding, A. de la Fuente Vornbrock, C. Ting, V. Subramanian, Patternable polymer bulk heterojunction photovoltaic cells on plastic by rotogravure printing, Sol. Energy Mater. Sol. Cells 93 (2009) 459–464.
[39] H.J. Park, M.-G. Kang, S.H. Ahn, and L.J. Guo, Facile route to polymer solar cells with optimum morphology readily applicable to roll-to-roll process without sacrificing high device performances, Adv. Mater., (2010) in press.
[40] K.X. Steirer, M.O. Reese, B.L. Rupert, N. Kopidakis, D.C. Olson, R.T. Collins, D.S. Ginley, Ultrasonic spray deposition for production of organic solar cells, Sol. Energy Mater. Sol. Cells 93 (2009) 447–453.